Plasmonic response of STM tips

Ping Chu and D. L. Mills*
Department of Physics, University of California, Irvine, California 92697, USA
(Received 11 April 2011; revised manuscript received 18 May 2011; published 15 July 2011)

We present theoretical studies of the plasmonic response of STM tips near substrates, with emphasis on the influence of tip shape and topology on its plasmonic resonances. The calculations employ COMSOL software. We find, for tips made of Ag, a plasmonic resonance in the 600–700 nm wavelength regime, which is well below the spectral range where one encounters surface and tip plasmons in electrostatic theory for Ag based structures. A similar low-energy resonance is found for Au tips. We present calculations of light emission spectra, wherein the light emission is stimulated by the noise necessarily present on a dc tunneling current. The calculated spectra are similar to those observed in recent experiments. We also discuss excitation of the low-frequency resonance by means of an external laser beam, and for both laser excitation and excitation by current noise we explore the relative strength of the low-frequency resonance and the "classical" tip/substrate plasmons in the 3.5 eV spectral range. The results suggest future experimental studies.

DOI: 10.1103/PhysRevB.84.045430 PACS number(s): 78.68.+m, 78.67.−n, 73.22.Lp, 68.37.Ef

I. INTRODUCTION

It has been known for decades that electrons in conducting media can exhibit collective resonant modes referred to as plasmons. These states can be excited in diverse ways, through use of electron or laser beams that impinge on a crystal or nanoparticle, or for that matter by any external probe that couples to the macroscopic electric field generated by the electron motions associated with these modes. Since plasmons seem ubiquitous, it is possible to design structures that support plasmons in desirable spectral regimes. Objects referred to as "nanoscrecsents" provide us with an interesting example of tunable structures under study currently.[1]

Excitation of plasmons by external laser beams can greatly enhance nonlinear optical signals from nanoscale to sub-nanoscale systems. That this is so was realized shortly after the discovery of the phenomenon of surface enhanced Raman scattering (SERS). It is argued that excitation of plasmons by both the incident and scattered photon involved in the Raman event produces very large enhancements of the signal, when the circumstances are appropriate.[2] Currently it is possible to observe Raman signals from single molecules by exploiting this effect.[3,4]

An STM tip will support surface plasmons, in a manner similar to those encountered in other metallic nanostructures. Since the tip is very close to a metallic substrate, the tip plasmons interact strongly with substrate surface plasmons to produce coupled modes of the tip/substrate complex.[5] These plasmons influence the physics encountered in the STM environment in diverse ways. For example, since such plasmons can be viewed as elementary excitations of the tip/substrate complex they necessarily undergo zero-point quantum fluctuations. We have demonstrated[6] that the interaction of electrons in molecules with such zero-point fluctuations lead to tip dependent energy level shifts and nonradiative lifetimes seen in STM studies of molecules,[7,8] when the adsorbates sit on an oxide layer that decouples their orbitals from direct overlap with those of substrate electrons. Also the plasmonic response of the tip/substrate complex plays an integral role in optical emission from such molecules, as illustrated by a comparison of theory and experiment.[9] Thus the collective plasmons of the tip/substrate enter importantly in diverse studies of molecules in the STM environment.

For purposes such as those just described, a theory based on a dielectric description would seem adequate. In such an approach, the various elements of the system are modeled as continua described by a complex, frequency dependent dielectric function. Since the linear dimensions of the region of interest are small compared with the wavelength of the relevant radiation, it is the case as well that an electrostatic description of the system response suffices for many purposes. Since the tip/sample separation is very small compared to the radius of curvature of a typical STM tip, in our past studies we have employed a model where the tip is replaced by a sphere, as discussed in Refs. 5 and 6 and papers cited therein. The plasmons of interest are localized very highly around the "south pole" of the tip so such a picture seems appropriate. Its virtue is that the electrostatic problem can then be solved in closed form through use of bispherical coordinates; zero-point fluctuations of the electromagnetic field in the vicinity of the tip and substrate can then be described as discussed by Abrikosov, Gor'kov, and Dzyaloshinskii.[10] This framework allows one to carry out very complex calculations such as those presented in Ref. 6.

The study reported in the present paper is motivated by very intriguing recent data.[11] The authors of Ref. 11 see a plasmon like peak in the spectrum of radiation emitted from a Ag tip placed above a NiAl substrate. This peak is evident as well in radiation emitted when a line of atoms under the tip is excited; while the presence of the adsorbate structure enhances the emission rate substantially, its spectral shape is rather similar to the case where tunneling current enters the bare substrate. What is striking is that this structure appears in the 1.75–2.00 eV (600–700 nm wavelength) regime, far to the red from the emission associated with plasmons localized near the Ag tip.

Possibly such a structure might be produced by a plasmon feature associated with the NiAl substrate. However this material is very lossy in this spectral region, as one sees from Fig. 3 of Ref. 12, so no plasmonic structure is expected. Indeed, theoretical studies of the plasmonic response of a Ag

tip placed above a NiAl substrate show no structure in the 600–700 nm spectral regime, when the tip is modeled as a sphere as discussed above.[13]

These considerations have led us to explore the plasmonic response of a model STM tip of realistic shape. We have done this for a tip placed above a substrate through the use of COMSOL software. In these simulations, we find plasmonic structures very similar to those that emerged in earlier studies based on the use of a sphere to model that part of the tip that is very close to the substrate. However, in addition for Ag tips we find a new collective excitation in the spectral range where the feature in Ref. 11 is reported. The frequency of this feature is controlled by the overall shape of the tip as we shall see, since its fields are far less localized at its end, when compared to those associated with the "tip plasmons" discussed earlier. We suggest that it is this collective mode that is responsible for the peaks in the emission spectrum reported in Ref. 11. Indeed, our studies of the shape of the emission spectrum when current is injected into the substrate compare very favorably with the data. A similar low-energy collective mode appears in our simulations of Au tips.

We shall present studies of the excitation of the tip collective mode just described for two distinct excitation mechanisms. The first is excitation by an incoming laser beam, and the second is excitation by a dc tunneling current between the tip and the substrate. In the latter case, as discussed many years ago in a closely related context,[14,15] there is noise necessarily present in the dc tunneling current, and within the framework of a semiclassical discussion, this noise is responsible for the radiation emitted when there is dc current between the tip and the substrate. We remark that this approach provides a very good account of both the spectral shape of the radiation emitted in the systems studied earlier, along with its absolute intensity.[14,15] In the Appendix, we provide a generalization of the simple form used earlier for the spectrum of noise associated with the tunneling current, and this forms the basis for our description of the emission spectrum. This expression may prove useful in other applications.

Our results suggest further experiments. First, the experiments in Ref. 11 employ maximum voltages of 2.6 eV. Since the maximum frequency in the single photon emission spectrum is $eV/\hbar$, a bias of 2.6 eV is too low to allow access to the Ag tip plasmons, which lie near the 3.5 eV range. Our calculations predict that current stimulated emission from the tip plasmons should be far more intense than that from the collective mode in the 600–700 nm regime that we suggest is responsible for the emission reported in Ref. 11. Thus, it would be highly desirable to extend experimental studies such as those reported in Ref. 11 to dc voltages above 3.5 eV, if possible. We show that the resonance in the 1.75–2.00 eV range and the tip plasmons in the 3.5 eV range may both be excited by an incident laser beam. Here the two sets of modes have comparable oscillator strength in regard to coupling to an incident laser beam. It would thus be of great interest to probe the response of the tip/substrate complex over a wide spectral range by optical means.

Our picture is that a Ag or Au STM tip near a substrate supports two distinct plasmonic mode structures. For Ag, the low-energy feature in the 2 eV range or below has fields that extend quite far from the tip region. This mode is sensitive to the overall tip topology and is rather insensitive to the nature of the substrate. There are then plasmons localized very near the tip, in the 3.5 eV range where diverse plasmon resonances associated with Ag based structures reside. These are affected by their interaction with the plasmonic response of the substrate. The former are rather weakly excited by noise fluctuations associated with dc current flow, by virtue of their delocalized nature, whereas the tip plasmons couple strongly. Conversely the low-energy feature couples well to an external laser beam, whose field also is delocalized whereas coupling to the high-energy tip plasmons is much weaker. A similar picture applies to Au tips; of course, for Au the effective bulk plasma frequency is much lower than in Ag so for Au the energy scale is different.

II. THE MODELING AND THE CALCULATIONS

We first discuss our means of modeling the STM tip. The COMSOL software requires that we utilize a description of its surface by analytic formulas. We proceed by setting up a truncated cone, within which an ellipsoid of revolution is embedded. The purpose of the ellipsoid is to remove the sharp singularity at the tip of a perfect cone. Also in our simulations we wish to probe the influence of variations in the radius of curvature of the tip on the various quantities we explore. We arrange the fitting so that the slope of the ellipsoid surface matches that of the cone surface along the ring of contact between the two shapes. This insures a surface with no discontinuities in slope, which is important if one is to achieve good convergence with COMSOL. In Fig. 1(a) we illustrate the overall shape we can achieve by this means, and in Fig. 1(b) we show how the prolate spheroid is nestled into the truncated tip of the cone and the resulting combination is parameterized.

The curvature R of the STM tip is determined by the choice of the semiaxes of the spheroid, a and b, given by $R = a^2/b$.

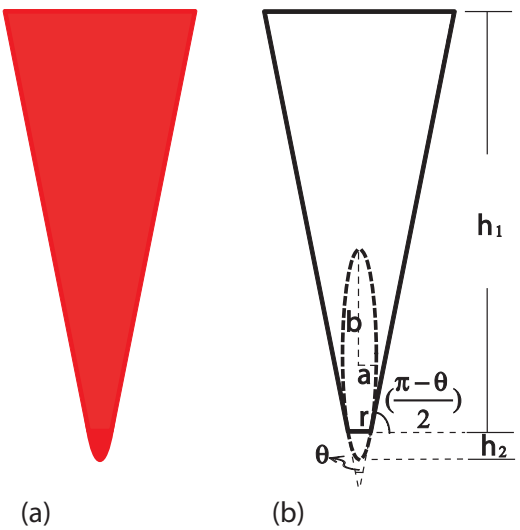

FIG. 1. (Color online) (a) The shape of a selected STM tip which results from the scheme described in the text. In (b) we show the parameters we use to describe the structure. The angle θ is the angle between the sides of the cone, and r is the radius of the opening at the point where the cone is truncated.

If h_2 is the height of the piece cut off of the tip and r is the radius of the hole so created at the tip of the cone, then these quantities satisfy

$$\frac{r^2}{a^2} + \frac{(b-h_2)^2}{b^2} = 1. \quad (1)$$

For the joint between the spheroid and the cone to be smooth, i.e., for the slopes of the surfaces to match, the following relation must be satisfied:

$$\frac{\theta}{2} = \frac{\pi}{2} - \tan^{-1}\left[\frac{b^2 r}{a^2(b-h_2)}\right]. \quad (2)$$

To set up the structure we explore in COMSOL 3.5, one can begin by drawing an ellipsoid with selected a and b with its bottom the distance d above the substrate, which is a flat plane. Typically we chose $d = 0.5\ nm$. We then chose the desired slope of the sides of the cone, as described by the choice of θ. Then from Eqs. (1) and (2) one can find values for both r and h_2 that insure the smooth fit described above. The height h_1 is always very large compared to h_2 so we have in the end a smooth conical shaped STM tip with a rounded tip of the desired curvature.

In the COMSOL simulation procedure, the objects to be studied are embedded in a finite domain, whereas open boundary conditions are applicable to the radiation problems of interest in our study. Since Maxwell's equations are integrated only over a finite domain, an issue is backscattered radiation from the boundary of the domain. One proceeds by surrounding the object studied with absorbing boundaries that eliminate backscattered radiation. The RF Module in COMSOL 3.5 offers two settings which may be used to optimize the absorption efficiency of the boundary, the scattering boundary condition and the perfectly matched layer (PML). The scattering boundary condition is applied at the outside boundary. A PML is an additional domain that absorbs the radiation incident on it with no reflection.[21] We illustrate the arrangement we have employed in our studies in Fig. 2. We remark that we have carried out extensive and lengthy convergence studies, to make certain that the results of interest are not affected by changes in how the structures at the boundary of the domain are arranged.

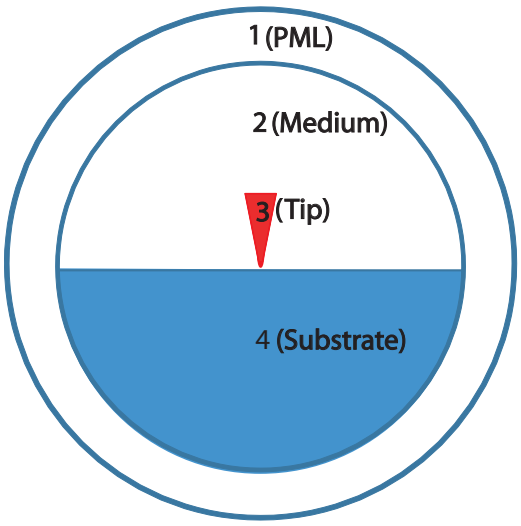

FIG. 2. (Color online) An illustration, not to scale, of the geometry we have employed in our simulations. Domain 1 is the PML and is vacuum. Its inner radius is 200 nm and outer radius is 250 nm. Domain 2 is the medium above the substrate and outside the tip, and this is vacuum. Domain 3 is the STM tip, and domain 4 is the substrate.

In our simulations, the tip is 0.5 nm above the substrate. An absorbing spherical shell with 200 nm radius and thickness of 50 nm encloses the structure, as illustrated in Fig. 2. We require the complex dielectric constants of Ag, Au, and NiAl, and these are found from Refs. 16 and 17. There is one point one should note with the COMSOL 3.5 software. The time dependencies for the fields are described by the convention $e^{+i\omega t}$ rather than the standardly employed $e^{-i\omega t}$, so the sign of the imaginary part of the dielectric constants must be taken to be negative, appropriate to negative frequencies.

III. NUMERICAL STUDIES OF THE PLASMONIC RESPONSE OF STM TIPS

Before we present our studies of the plasmonic response of STM tips, we wish to provide a comparison of our simulations with those in earlier work, to illustrate that we have achieved very good convergence in our studies. Hao and Nordlander have explored the plasmonic response of Ag nanoshells through the use of FTDT software which employs an algorithm qualitatively different from COMSOL. These authors also have employed various other numerical packages as well.[18] In their Fig. 4(b) they provide a spectrum of such a structure with internal radius of 80 nm, outer radius of 100 nm, and a silica core; the spectrum is quite complex in nature. In our Fig. 3(a), we show our COMSOL simulation of the same object, and in Fig. 3(b) we reproduce their result. The FTDT simulation is the black curve, and the two calculations agree well as one can see.

We now turn to our studies of STM tips. In what follows, the figures display the electric field just below the tip, which is linearly related to the radiative field in the far zone. In all figures the tip is 0.5 nm above the substrate. We have chosen the parameters that describe the geometry of the tip to provide a close approximation to images of actual STM tips.[19] We use $\theta = 40^\circ$, $r = 0.32$ nm, $h_2 = 0.42$ nm, and $h_1 = 15$ nm.

In Fig. 4, we show a sequence of simulations of the response of a Ag tip above a NiAl substrate. In Fig. 4(a) we have laser excitation of the tip, where the laser beam propagates parallel to the substrate, with electric field perpendicular to the substrate. In the vicinity of 3 eV, we see plasmonic structures qualitatively similar to those displayed in earlier work (Ref. 6). The structure near 2 eV is the collective mode that is the focus of the present study. We refer to this as the low-frequency plasmon, and the modes near or above 3 eV will be designated as tip plasmons. In Fig. 4(b), for the same tip, substrate, and tip/substrate separation, we show the frequency spectrum of the electric field just under the tip in response to current excitation. In this calculation, we have taken the Fourier amplitude I_ω^2 of the current fluctuation (see the Appendix) to be frequency independent, to focus attention on the plasmonic response of the tip. We see a Ag tip plasmon near 3.5 eV, and no low-frequency structure can be seen on the scale used in Fig. 4(b). It is the case, however, that the signature of the

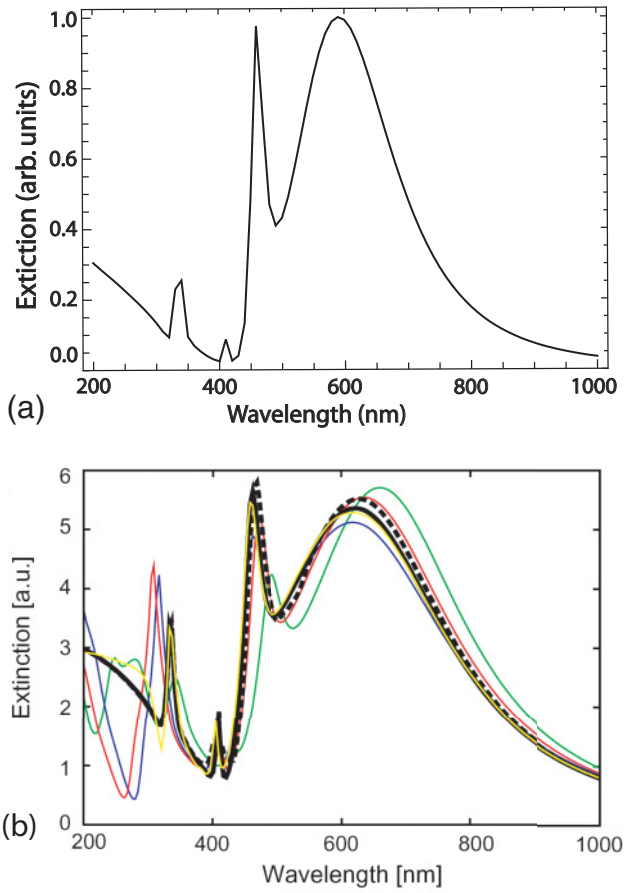

FIG. 3. (Color online) In (a), we show our COMSOL simulation of the plasmonic response of a Ag nanoshell with inner radius of 80 nm and outer radius of 100 nm and a silica core with a permittivity of 2.04. The shell is excited by an incident plane wave whose amplitude is constant as frequency is varied, and as in Ref. 18 we calculate the extinction rate. In (b), we reproduce Fig. 4(b) from Ref. 18 (with permission) which may be compared with our work. Several software packages have been used in this paper. The black curve is the FTDT simulation that is fully converged. We refer the reader to Ref. 18 for further discussion.

low-energy collective mode is indeed present. It is just that current excitation excites this mode only weakly. We illustrate this in Fig. 4(c), where the spectrum displayed in Fig. 4(b) is plotted on a logarithmic scale. What is happening is that current excitation couples strongly only to plasmon modes localized in the very near vicinity of the tip, whereas in laser excitation the entire tip is illuminated so that modes with fields spread over a larger area are coupled to more strongly than those right at the point of the tip.

We illustrate this last point in Figs. 5 and 6, where we illustrate the field distributions associated with the prominent features in Fig. 4. Figure 5 describes the field patterns excited in current excitation. We see that the very strong tip plasmon whose signature appears just above 3.5 eV in Figs. 4(b) and 4(c) has fields highly localized around the end of the STM tip, whereas the much weaker mode near 2.1 eV has its fields distributed over the whole lower part of the structure. A consequence of this is that the properties of the low-frequency

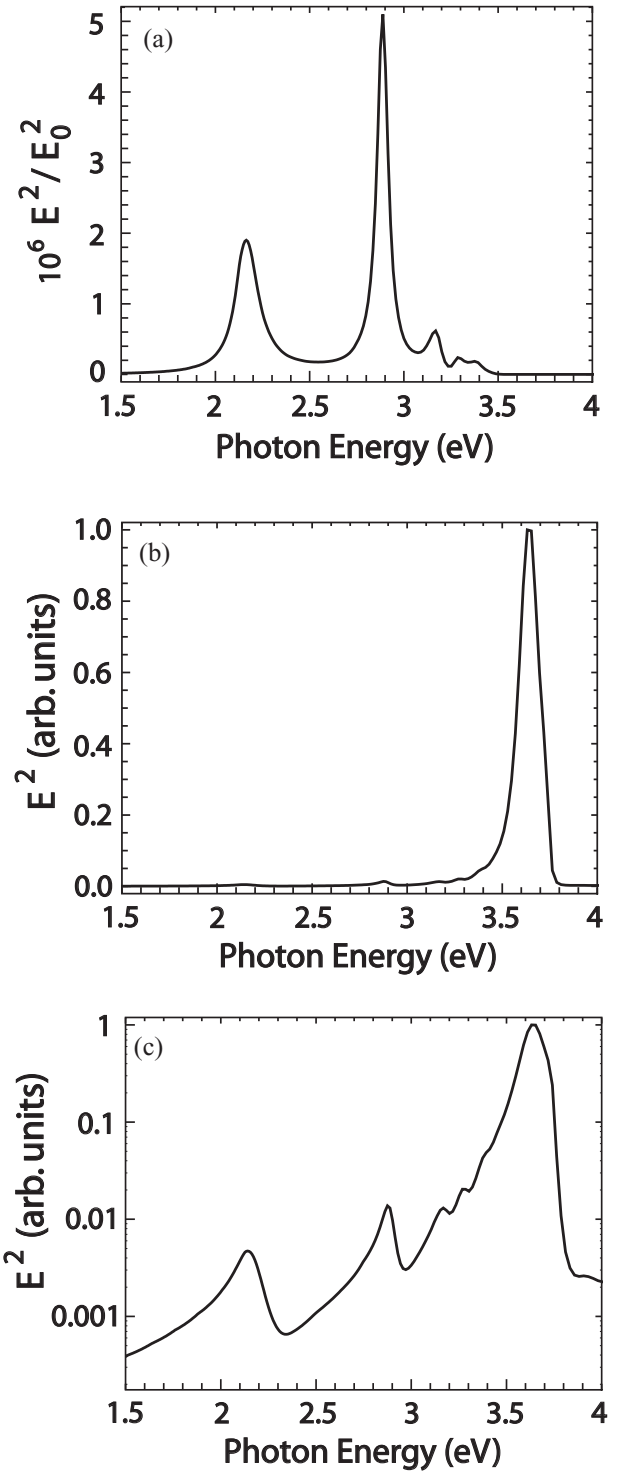

FIG. 4. We show the scattered electric field spectra under the STM tip in (a) laser excitation (the propagation is along the substrate surface and the polarization is normal to the surface), and (b) and (c) show current excitation, where (c) is identical to (b) but with a logarithmic scale. The parameters of the Ag tip are given by the semiaxes $a = 0.8$ nm, $b = 5$ nm, the semiangle of the cone $\theta/2 = 20^\circ$, the bottom radius of the cone $r = 0.32$ nm, the height of the end tip $h_2 = 0.42$ nm, and the height of the cone $h_1 = 15$ nm. The separation between the tip and the substrate NiAl is 0.5 nm.

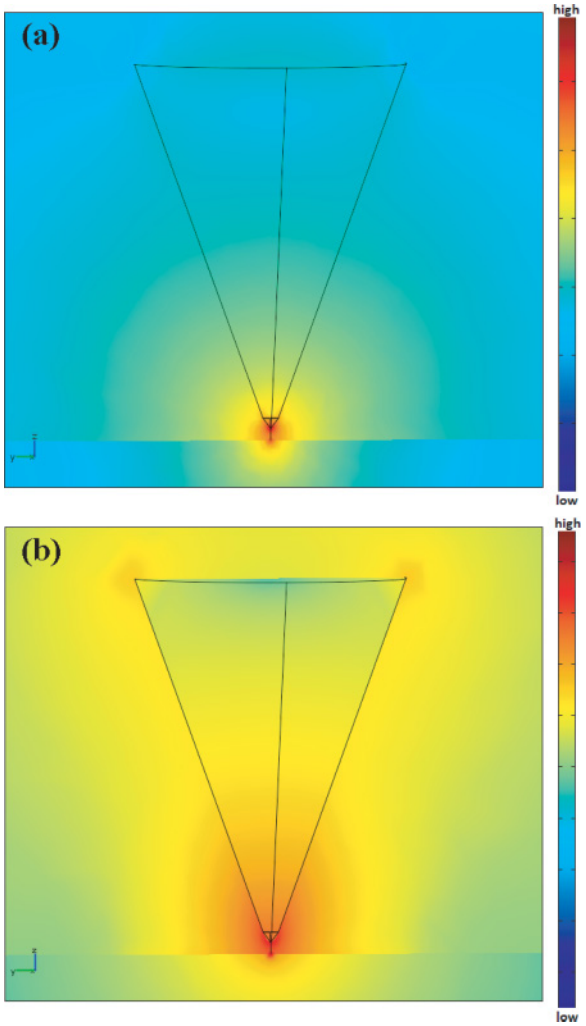

FIG. 5. (Color online) We show the intensity of the electric field between the STM tip and the substrate excited by current excitation. The photon energy is 3.6 eV in (a) and 2.1 eV in (b). The parameters of the silver tip are the same as in Fig. 4.

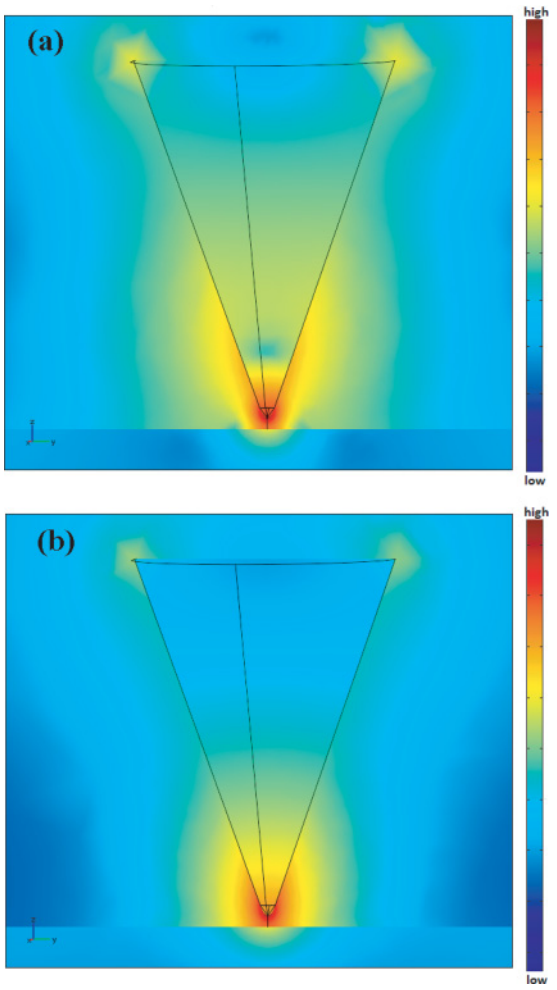

FIG. 6. (Color online) We show the spatial distribution of the scattered electric field intensity between the STM tip and the substrate in z-polarized laser excitation. The photon energy is 2.9 eV in (a) and 2.1 eV in (b). The parameters of the silver tip are the same as in Fig. 4.

mode are sensitive to overall topology of the tip, as we illustrate below. Tip plasmons will lie very close in energy to the Mie resonance of a very small sphere; in electrostatic theory the position of the Mie resonance is independent of the radius of the sphere so the qualitative features in the tip plasmon region are not so sensitive to the overall shape of the tip.

In Fig. 6, we show the spatial distribution of fields with the two prominent modes present in Fig. 4(a), which describes laser excitation of the system. The mode near 3.6 eV, whose fields are tightly compacted at the tip as we see in Fig. 5(a), is only excited very weakly by the laser beam. The prominent structure just below 3 eV in Fig. 4(a) is a mode whose fields extend farther from the near vicinity of the tip, as illustrated as Fig. 6(a).

In Fig. 7, we show calculations of laser stimulated plasmonic response of tips modeled as in Refs. 5 and 6. Recall, as mentioned above, that the tip is modeled in these discussions as a sphere placed a bit above the substrate. For a Ag tip above a NiAl substrate modeled in this manner we see plasmonic structures qualitatively similar to those illustrated above in the tip plasmon regime of 3 eV and above. However, the low-energy collective mode that is the focus of the present paper is missing. Note that as the radius of curvature of the tip increases, the most prominent feature in Fig. 7 drops in frequency. For current excitation of the plasmons of the tip/substrate combination the simple model is adequate in our view, but for laser excitation the low-frequency plasmon mode asserts itself strongly as we see from Fig. 4(a).

We turn now to calculations directed toward the data that have motivated the present study. The remaining figures employ COMSOL simulations of current excitation, with the current noise spectrum described by Eq. (A4) and the model of the tip that described in the caption of Fig. 4. We have used a typical I-V curve taken from Ref. 19 for these calculations. In Fig. 2(a) of Ref. 11 we see a spectrum taken over the bare NiAl surface with a dc bias voltage of 2.6 eV. The experimental curve is quite similar to the red dashed curve in Fig. 8(a). The prominent structure just above 2.1 eV in Fig. 8(a) for a bias voltage of 2.6 eV agrees well with the principal peak in the data. There is a shoulder in the data above the main peak we do not see in the theory. However, while the spectra taken with diverse tips are similar in nature,[19] there are differences

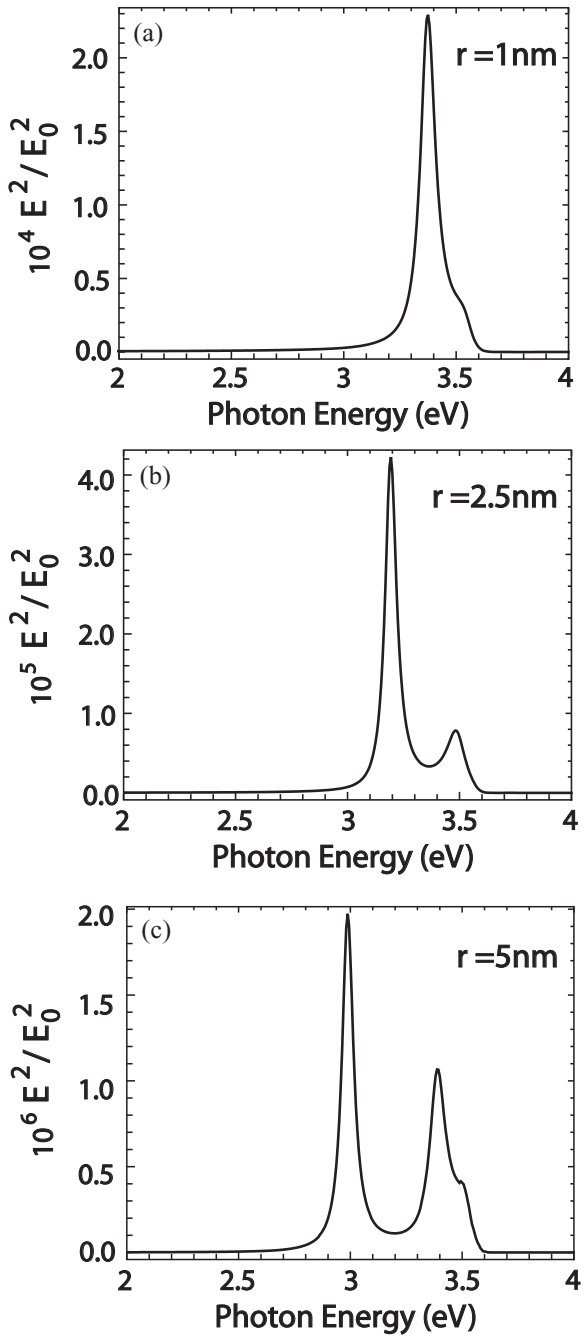

FIG. 7. The plasmonic response of three Ag spheres placed 0.5 nm above a NiAl substrate, for three different choices of sphere radii. The system is excited by a spatially uniform external field applied perpendicular to the substrate. The plots show the intensity of the electric field just below the sphere, normalized to that of the incident field. The calculations are performed in the electrostatic limit, by means of the method discussed in Refs. 5 and 6.

in details in the experimental spectrum from tip to tip. Note that if the bias voltage is increased to 3 eV, in the theory we begin to see the onset of the very strong tip plasmon emission displayed in Fig. 4(b) above. Clearly for current stimulated emission, we predict that one will see very strong emission in the tip plasmon regime around 3.5 eV or so. It would be of great interest to see measurements that explore this regime.

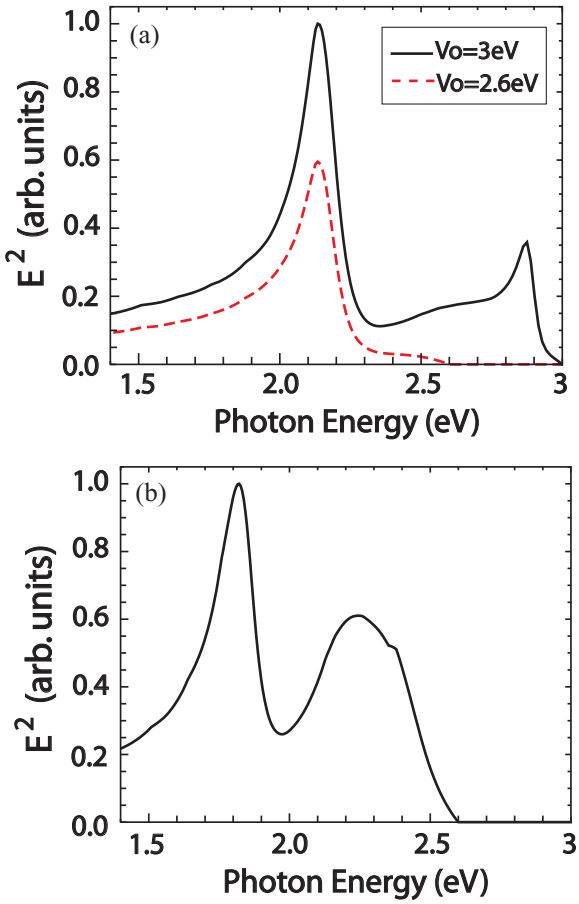

FIG. 8. (Color online) Calculations of the current driven emission spectrum for (a) a Ag tip 0.5 nm above a NiAl substrate, for the two dc bias voltages indicated, and (b) for a Au tip placed 0.5 nm above a NiAl substrate, for a bias voltage of 2.6 eV.

In Fig. 8(b), we see calculations for a Au tip placed above a NiAl substrate, for a dc bias of 2.6 eV. The low-energy plasmon has now shifted down in frequency, and we see a broad emission in the Au plasmon regime just below 2.5 eV. The Au tip plasmons, rather heavily damped in this material, are accessible with voltages such as those used in Ref. 11.

The calculations for the STM tip presented above use the model description of the tip described in the caption of Fig. 4. As noted above, the properties of the low-energy mode are sensitive to the overall topology of the tip. We illustrate this in Fig. 9(c), where for a dc bias voltage of 2.6 eV we compare the emission spectrum for tips of the two different cone angles illustrated in Figs. 9(a) and 9(b). We see that as the tip becomes "fatter" the frequency of the low-frequency mode increases. The tip with the larger cone angle of forty degrees produces an emission spectrum [Fig. 9(c)] which appears to agree well with the data of Ref. 11. The tip profile in Fig. 9(a) is qualitatively similar to the tips illustrated in Ref. 9, although of course we cannot say how this figure compares in detail with the tip used in the actual experiment.

The nature of the substrate has rather little influence on the frequency of the low-energy peak. However, it can affect the shape of the spectral feature, since the fields associated with the collective mode couple to electrons in the substrate with

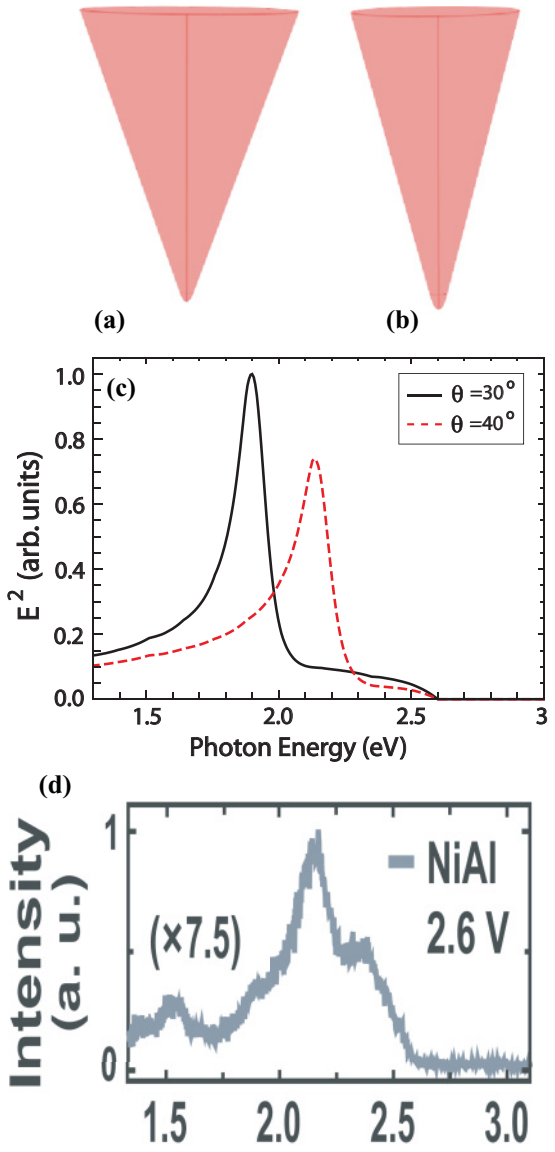

FIG. 9. (Color online) In (c) we illustrate the current driven emission spectrum for the two tips illustrated in (a) and (b), for a dc bias voltage of 2.6 volts. The red dashed curve is the spectrum for the tip in (a) and this tip is the same as that used in earlier figures. The black solid curve is for a tip whose cone angle is 30°, as illustrated in (b). For this tip, $r = 0.41$ nm, $h_2 = 0.71$ nm, and $h_1 = 15$ nm. In (d), we show the experimental spectrum of radiation emitted from a Ag tip above a NiAl substrate. The data in (d) are reproduced from Ref. 11, with permission.

the consequence that the width of the peak is affected by the dissipation rate in the substrate. We illustrate this in Fig. 10, where for the Ag tip utilized in the calculations presented in Fig. 4 we compare the emission spectrum when the tip is over a (quite lossy) NiAl substrate with that when a Au substrate is used.

IV. CONCLUDING REMARKS

In this paper, we have presented COMSOL simulations of the plasmonic response of STM tips above a substrate, wherein

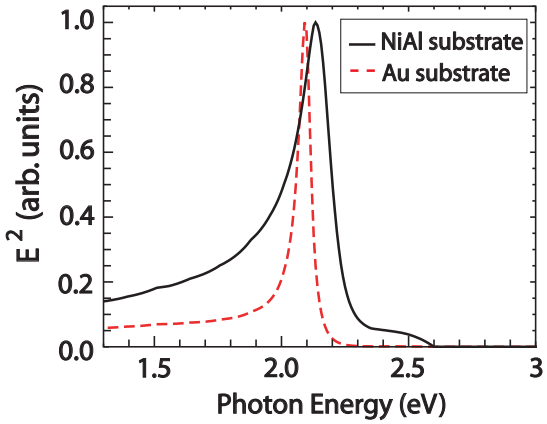

FIG. 10. (Color online) For a dc bias voltage of 2.6 eV, we show the current driven emission spectrum when a tip with cone angle of 40° is placed 0.5 nm above a NiAl substrate (black solid curve) and over a Au substrate (red dashed curve). The tip is described by the parameters given in the caption of Fig. 4.

the tip has a realistic shape. We find substantial differences between two means of exciting plasmonic modes of the tip/substrate combination: excitation by an external laser beam, and excitation via the noise necessarily present when a dc current flows between tip and substrate. For laser excitation, the plasmon modes excited are those that have fields which extend well beyond the tip region itself. We find a low-energy plasmon mode that appears prominently in the laser excited spectrum well removed from the energy range associated with plasmons localized near the tip. In contrast, current excitation excites tip plasmons most prominently, although the low-energy mode is indeed present as a weak feature. Our calculations suggest that it is current excitation of the low-energy feature that is responsible for the structure reported in Ref. 11.

If this is the case, then we predict that for Ag tips, much more intense radiation should be found if the dc voltage can be extended above 3.5 eV, where current noise couples strongly to the localized tip plasmons. It would also be of great interest to compare the spectrum of radiation emitted with current and laser excitation of the same tip, to explore the differences evident in our theoretical simulations. It is our hope that the discussion presented above will stimulate new experimental studies of the plasmonic response of STM tips in the near vicinity of substrates.

ACKNOWLEDGMENTS

We wish to thank Wilson Ho and Chi Chen for numerous stimulating discussions during the course of this research. The research was supported by the US National Science Foundation under Grant No. CHJE-0802913.

APPENDIX: DESCRIPTION OF NOISE ASSOCIATED WITH THE DC TUNNELING CURRENT

In the text it is argued that in the presence of the dc current, noise is necessary associated with the current. It is this noise that leads to the light emission. Many years ago, the Bardeen tunneling Hamiltonian was employed[20] to argue

that the spectrum of this noise is proportional to $(1-\hbar\omega/eV_0)$ with ω the frequency of interest and V_0 the applied dc voltage. This form was utilized in earlier theories of light emission from classical tunnel junctions[15] and also for tunneling from oxidized metal surfaces into small particles.[14] The simple form just quoted is derived under the assumption that the density of states in both metals involved in the tunneling process is structureless. For the large voltages and materials used in Ref. 11 this assumption breaks down badly, since the *I-V* curve is highly nonlinear. This Appendix is devoted to generalizing the expression obtained in Ref. 20. We shall arrive at a very simple final expression.

We consider states in the STM tip labeled by quantum numbers that we refer to by the symbol α and states in the substrate labeled by quantum numbers β. We write the Bardeen Hamiltonian in the form

$$V=\sum_{\alpha,\beta}\{Tc_\alpha^+c_\beta+T^*c_\beta^+c_\alpha\}, \tag{A1}$$

where, following Ref. 16, our principal approximation is to ignore the details of the tunneling matrix element and its dependence on the states involved in the tunneling process. Let $N_{Tip}(\varepsilon)$ be the density of states of the tip, with ε measured from the Fermi level of the tip, and let $N_{Sub}(\varepsilon')$ be the density of states of the substrate, with ε' measured from the Fermi level of the substrate. Suppose the dc voltage V_0 is such that electrons flow from the tip into the substrate. Then a standard calculation shows that the dc current is given by (at zero temperature)

$$I_{dc}(V_0)=2\pi e|T|^2\int_{-eV_0}^{0}d\varepsilon N_{Tip}(\varepsilon)N_{\rm Sub}(\varepsilon+eV_0). \tag{A2}$$

To evaluate the frequency spectrum of the current noise, we study the expectation value $\langle I(t)I(0)\rangle=\int_{-\infty}^{+\infty}\frac{d\omega}{2\pi}I_\omega^2e^{-i\omega t}$ where for our model Hamiltonian the current operator is $I=ie\sum_{\alpha,\beta}\{Tc_\alpha^+c_\beta-T^*c_\beta^+c_\alpha\}$. In the correlation function, the operators are in the Heisenberg representation. At the absolute zero of temperature, after some calculation we find that

$$I_\omega^2=2\pi e^2|T|^2\theta(eV_0-\hbar\omega)\int_{-(eV_0-\hbar\omega)}^{0}d\varepsilon N_{Tip}(\varepsilon)\times N_{\rm Sub}(\varepsilon+eV_0-\hbar\omega), \tag{A3}$$

where $\theta(x)$ is the Heaviside step function. Thus we have the remarkably simple relation

$$I_\omega^2=e\theta(eV_0-\hbar\omega)I_{dc}(V_0-\hbar\omega/e). \tag{A4}$$

Then the frequency spectrum of the noise associated with the tunneling current is controlled by the dc *I-V* curve, which is well known for any particular junction. If the *I-V* curve is linear in voltage, then Eq. (A4) becomes simply

$$I_\omega^2=\frac{e}{R}\theta(eV_0-\hbar\omega)(V_0-\hbar\omega/e), \tag{A5}$$

where $R=V/I$ is the resistance of the junction.

The expression in Eq. (A5) agrees with Eq. (3) of Ref. 20; the factor of 2π in the denominator of their expression has its origin in a different convention in the definition of I_ω^2. The junctions used in the experiments reported in Ref. 11 have a highly nonlinear *I-V* characteristic in the regime of voltage of interest to the present study, as one can appreciate from Fig. 2(D) in Ref. 11. Thus, Eq. (A4) provides a generalization of Eq. (A5) that we can use in the presence of strong nonlinearities in the *I-V* characteristics.

*dlmills@uci.edu

[1] Rostislav Bukasov, Tamer A. Ali, Peter Nordlander, and Jennifer S. Shumaker-Parry, ACS Nano **4**, 6639 (2010).

[2] M. Moskovits, Rev. Mod. Phys. **57**, 783 (1985).

[3] S. Nie and S. R. Emory, Science **275**, 1102 (1997).

[4] J. Jiang, K. Bosnik, M. Maillard, and L. Brus, J. Phys. Chem. B **107**, 9964 (2003).

[5] For a discussion of collective plasmons of the STM tip/substrate complex, see D. L. Mills, Phys. Rev. B **65**, 125419 (2002); Shiwei Wu and D. L. Mills, *ibid*. **65**, 205420 (2002).

[6] Ping Chu and D. L. Mills, Phys. Rev. B **79**, 115435 (2009).

[7] G. V. Nazin, S. W. Wu, and W. Ho, Proc. Natl. Acad. Sci. USA **102**, 8832 (2005), See Fig. 4(b).

[8] S. W. Wu, G. V. Nazin, and W. Ho, Phys. Rev. B **77**, 205430 (2008).

[9] Chi Chen, Ping Chu, C. A. Bobisch, D. L. Mills, and W. Ho, Phys. Rev. Lett. **105**, 217402 (2010).

[10] A. A. Abrikosov, L. P. Gor'kov, and I. E. Dzyaloshinskii, *Methods of Quantum Field Theory in Statistical Physics* (Prentice Hall, Englewood Cliffs, NJ, 1963), See Chap. 6.

[11] Chi Chen, C. A. Bobisch, and W. Ho, Science **325**, 981 (2009).

[12] D. L. Mills, J. X. Cao, and Ruqian Wu, Phys. Rev. B **75**, 205439 (2007).

[13] See Fig. 4 of Ref. 6.

[14] R. W. Rendell, D. J. Scalapino, and B. Muhlschlegel, Phys. Rev. Lett. **41**, 1746 (1978).

[15] B. Laks and D. L. Mills, Phys. Rev. B **20**, 4962 (1979).

[16] P. B. Johnson and R. W. Christy, Phys. Rev. B **6**, 4370 (1972).

[17] For these calculations, we require both the real and the imaginary parts of the frequency-dependent dielectric constant of NiAl. In the literature, one finds only data on the imaginary part (or, equivalently, the real part) of the conductivity. We are grateful to Joo Rull Yee for providing us his data on both the real and the imaginary parts of the optical dielectric constant of NiAl.

[18] F. Hao and P. Nordlander, Chem. Phys. Lett. **446**, 115 (2007).

[19] Chi Chen, Ph.D. thesis, University of California, Irvine, 2009. This document is available online.

[20] D. Hone, B. Muhlschlegel, and D. J. Scalapino, Appl. Phys. Lett. **33**, 203 (1978).

[21] For the interested reader, a description of the software package we use can be found at [http://www.comsol.com/products/rf/].